



STScI | SPACE TELESCOPE
SCIENCE INSTITUTE

Instrument Science Report WFC3 2018-10

Updates to the *WFC3/UVIS* Filter-Dependent and Geometric Distortions

C. Martlin, V. Kozhurina-Platais, M. McKay, E. Sabbi.

July 11, 2018

ABSTRACT

Individual geometric distortion solutions and fine-scale filter distortion solutions are now available for many narrow band, medium band, and unique band UVIS filters. The main result of calibration proposal 14393 are a set of new polynomial coefficients for 20 previously uncalibrated UVIS filters. These high-order solutions are available in the form of an Instrument Distortion Coefficient Table (IDCTAB) while a set of new 2D look-up tables (NPOLFILES) are also available to correct for filter-distinct distortions. These reference files are used by the STSDAS software in the HST pipeline and in DrizzlePac/AstroDrizzle to correct for the distortions in WFC3/UVIS images. Distortions can now be successfully corrected to the level of ~ 0.05 pixel for the vast majority of filters, which is an improvement from previous levels of ~ 0.10 pixel. We investigate the effects of these filter dependent linear distortions and filter wedges through the relative plate scales and X, Y centroid shifts of each filter.

1. Introduction

There have been many extended studies following the original SMOV (Servicing Mission Orbital/Observatory Verification) investigation prior to launch, which solved for the geometric distortions due to the optical arrangement of the Hubble Space Telescope. It is well-known that there are strong distortions up to $\sim 5''$ in the UVIS detector, and previous studies by Kozhurina-Platais *et al* (2009,2012,2014) have described how to correct WFC3/UVIS images for the optical distortion. The same techniques have been used here to derive the high-order polynomial coefficients as were used in these previous reports.

Furthermore, as described in Kozhurina-Platais *et al* (2014), there is also a fine-scale distortion consisting of systematic residuals remaining after applying the best-fit polynomial solutions. These fine-scale systematic residuals cannot be removed by a polynomial model like the geometric distortions can be. These fine scale distortions result from the combination of a detector flaw caused by the manufacturing process and imperfections of the individual filters themselves. The removal of the offsets due to the detector flaws is done with a single 2D look-up table (D2IMFILE) (Kozhurina-Platais *et al* 2013). The remaining offsets introduce additional systematics in each set of filter-dependent distortion corrections. These systematics are on the order of ~ 0.05 to ~ 0.1 UVIS pixels and the fine-scale residuals are different for different filters. Therefore filter-dependent distortion patterns should be calibrated for by deriving 2D look-up tables for individual filters to use during image processing with *DrizzlePac/AstroDrizzle*.

The purpose of this paper is three-fold. We derived unique high-order polynomial solutions for the geometric distortions of 20 UVIS filters that previously had no solutions: F280N, F343N, F373N, F390M, F398N, F469N, F475W, F475X, F478N, F502N, F547M, F600LP, F631N, F645N, F656N, F658N, F665N, F680N, F763M, F845M; as well as individual 2D look-up table solutions for the filter-dependent fine-scale distortions for those same 20 UVIS filters. We demonstrate how the unique solutions provide an improvement for aligning images taken in different filters through an investigation into the X, Y residuals left after individual distortion corrections. We finish with an investigation into the effects of filter dependent linear distortions and filter wedges through a presentation of the relative plate scales, the X, Y specific centroid shifts and the general centroid shifts.

2. Observations

Both the high-order polynomial solutions and the 2d look-up table solutions for all filters were created using observations of Omega Centauri (ω Cen). These solutions are, as before, based upon the astrometric catalog of ω Cen used and described in Kozhurina-Platis, *et al.* 2009, 2012, 2014.

All filters were used to take observations near the center of the astrometric standard field with a mostly $+40.0/-40.0$ dither pattern and reference images in F606W were taken shortly after each uncalibrated filter. The observations for these calibrations can be found in the following HST calibration proposals: (1) PI: Kozhurina-Platais, CAL-14393, (2) PI Kozhurina-Platais,

CAL-14301, (3) PI Sabbi, CAL-11922, and (4) PI: Wong, 12091. Further information about individual observations, such as exposure time, individual file names and POSTARG values which show the dither pattern can be found in Appendix A.

3. Reductions

The methods used to create the high order polynomial solutions of the geometric distortions and the 2D look-up tables of the filter-dependent distortions have both been discussed at length in Kozhurina-Platais, *et.al* 2009, 2014. For further information on the methods used please reference those discussions.

The analysis completed in this paper is an extension to the recent results published in Kozhurina-Platais, *et.al* 2009, 2014. In 2014, 14 most popular UVIS filters were fit with individual geometric distortion solutions and here we expand that to another 20 UVIS filters. For those 14 UVIS filters there were also a set of fine-scale low amplitude distortions which are caused by the manufacturing process of the filters themselves. We replicated the process of creating a 2D-lookup table to correct for these imperfections for all 20 UVIS filters we updated. All geometric distortion solutions for individual UVIS filters are available through the HST-pipeline in a single reference file called the IDCTAB. The solutions for the fine-scale filter distortions are available in individual NPOLFILES, also through the HST-pipeline. The newest updates to the IDCTAB and the NPOLFILES for all 20 UVIS filters have been delivered to the Calibration Database System (CRDS) as a part of this study.

4. Verifying Individual Distortion Solutions

Following the updated calibration of 20 *UVIS* filters, we completed checks of all new solutions using the STSDAS software *TweakReg* which is a subpackage in *DrizzlePac/Astrodrizzle*. This set of packages is used to align and combine HST images for better spatial resolution. While we will go into some detail on the subpackage *TweakReg*, further information about *DrizzlePac/Astrodrizzle* can be found in the *DrizzlePac/Astrodrizzle* Handbook, 2012.

Our main verifications were completed with *TweakReg* which uses `*_flc.fits` files as input then finds X and Y positions of sources in the images before using the distortion reference files (such as our updated geometric and filter-dependent solutions) provided by the file headers under IDCTAB and NPOLFILE to correct those positions. *TweakReg* also solves each image match for the shift and rotation between them. We mainly use the residuals from the X and Y position matches found by *TweakReg*. We compare the residuals from one run (using the reference F606W geometric solution for both images and the residuals found by *TweakReg*) with those from a second run (using individual geometric distortion solutions for both images) to see whether the individual solutions improved the systematic trends and RMS of the X,Y solutions.

All sets of *TweakReg* residual plots can be found in Appendix B, and a prime example of them can be found below in Figure 1. This example demonstrates how we first ran *TweakReg* on a set of images using the reference F606W geometric solutions on both our F606W image

and on our specific filter image. The plot on the left shows how using the geometric solutions of F606W for all filters can lead to dramatic systematic errors and a high RMS in X,Y. Once we had updated our calibration for F656N we ran *TweakReg* on the F606W and F656N images, this time applying the F606W geometric solution only to the F606W image and our newly derived solution for F656N to that image. The plot on the right illustrates the power of a unique filter-dependent geometric and fine-scale solution. We can see how the newly-derived reference files improved the RMS of the solution from about 0.1 pixel to 0.05 pixel and greatly decreased the systematics of the X,Y residuals.

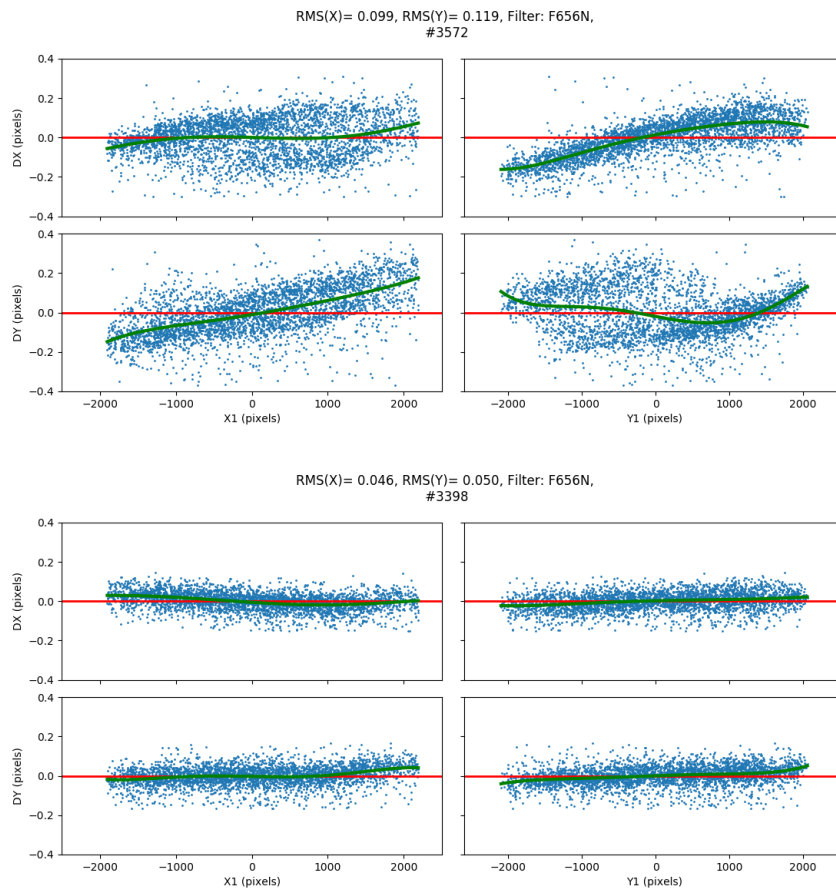


Figure 1: **Top:** TweakReg residuals for the matching of stars in the same image of ω Cen taken with F606W and F656N solved using the F606W solution for both images. **Bottom:** TweakReg residuals for the matching of stars in the same image of ω Cen taken with F606W and F656N solved using the proper distortion solution for each filter. Both plots provide RMS solution and star count information at the top.

5. Results

5.1 Relative Plate-Scales: X&Y Scales

We studied the differences in relative plate scales of each filter from that of our reference filter F606W to help investigate the range of distortions caused by the differences in filter manufacturing. We first normalized the relative X,Y plate scales of each filter to the relative plate scale of F606W (Eq. 1 and 2).

$$\Delta X_{scale_filter} = (X_{scale_filter} - X_{scale_{F606W}}) \quad (1)$$

$$\Delta Y_{scale_filter} = (Y_{scale_filter} - Y_{scale_{F606W}}) \quad (2)$$

Figure 2 has these differences in plate scales for both *UVIS* chips with the X-scales of each filter in the top plot and the Y-scales of each filter in the bottom plot. We can see across changing central wavelengths of each filter that the X-scale and Y-scale both vary from the reference filter X and Y-scales by as much as 0.0004. The absolute *UVIS* plate scale used by the *DrizzlePac/AstroDrizzle* software is 0.04 arcsec/pixel (Fruchter, 2009), making this variation cause a difference of up to 0.01 pixels between filters.

5.2 Filter Wedge: X&Y Centroid Shifts

A study on the *UVIS* filter wedge was published on in Sabbi, 2012. The study discussed how various glass layers of a filter may not be coplanar and can therefore introduce positional offsets for sources in images. The quantification of these offsets is called the filter wedge. After the creation of 2D look-up table solutions for the filter-dependent distortions for each *UVIS* filter we decided to investigate the dependence on filter of the measured X-offset and Y-offset, which can also be referred to as the centroid shifts. We have included how we calculated the normalization of each filter to the reference values of F606W for our plots (Eq. 3 and 4).

$$\Delta X_{shift_filter} = (X_{shift_filter} - X_{shift_{F606W}}) \quad (3)$$

$$\Delta Y_{shift_filter} = (Y_{shift_filter} - Y_{shift_{F606W}}) \quad (4)$$

In the top plot in Figure 3 below, one can see the Y-offset vs. filter and in the bottom plot of Figure 3 one can see the X-offset vs. filter, with respect to F606W. The measured Y shift for each filter is in the range of 0.40 to -0.60 from that of the reference F606W value; while the X shift per filter is in the range of 0.10 to -0.16 from that of the reference F606W value. We see higher shifts in the Y-offset than the X-offset, which was also seen in Sabbi, 2012, but neither was expected to have a systematic trend across wavelengths. These offset values are a powerful diagnostic of the filter wedge differences; we expected variation across filters due to the manufacturing differences, and do see that in our results.

5.3 Filter Wedge: General Centroid Shifts

Lastly we investigated the general centroid shift of each filter, as done previously in Sabbi (2012). In Sabbi (2012) this value is referred to as the "Shift" and can be found in the table

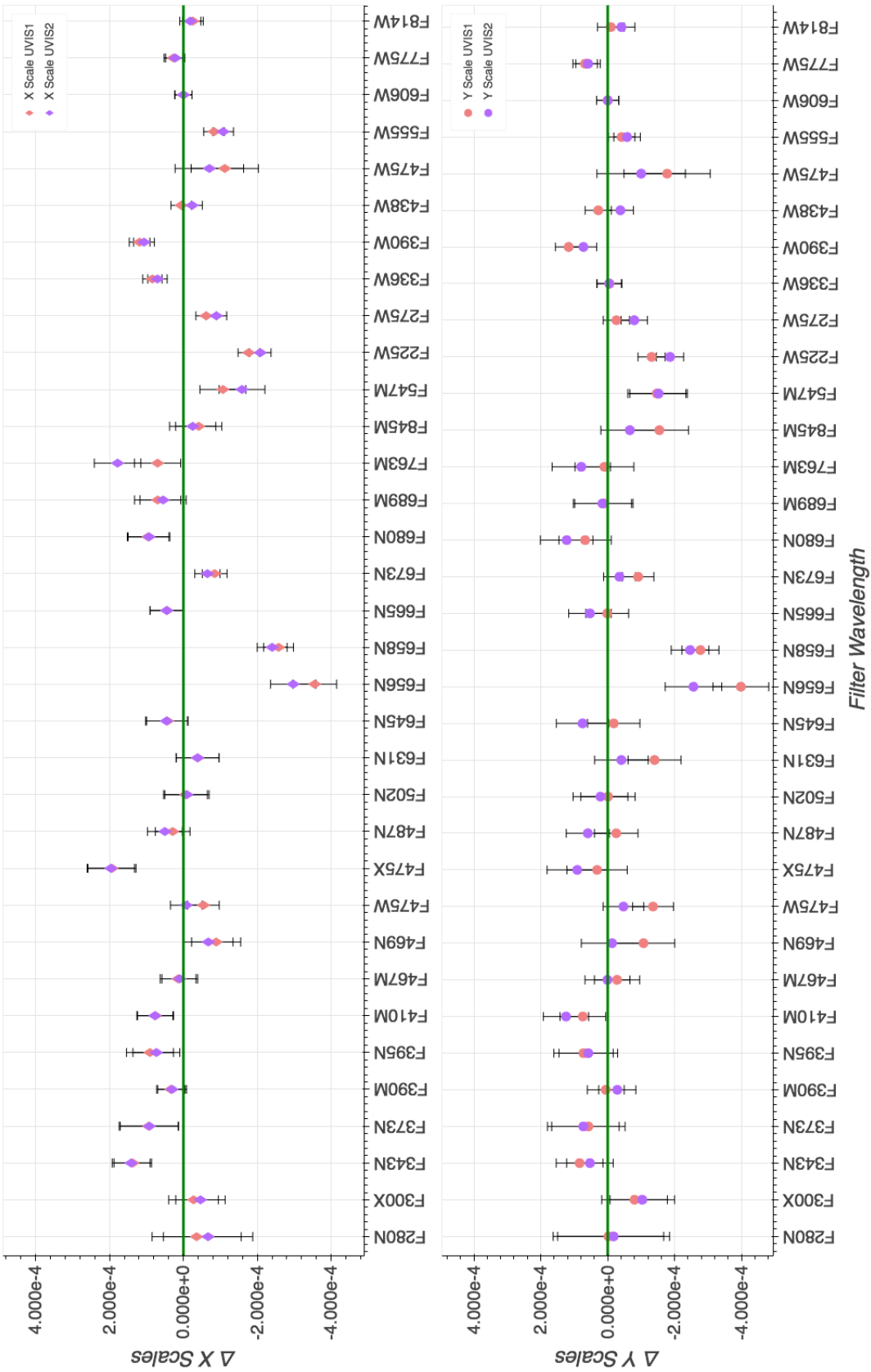


Figure 2: Plate scale values for every filter for UVIS 1 and UVIS 2. The **(top)** plot has ΔX -Scale values for both chips as normalized to the reference X-Scale of F606W. The **(bottom)** plot has the ΔY -Scale values for both chips as normalized to the reference Y-Scale of F606W.

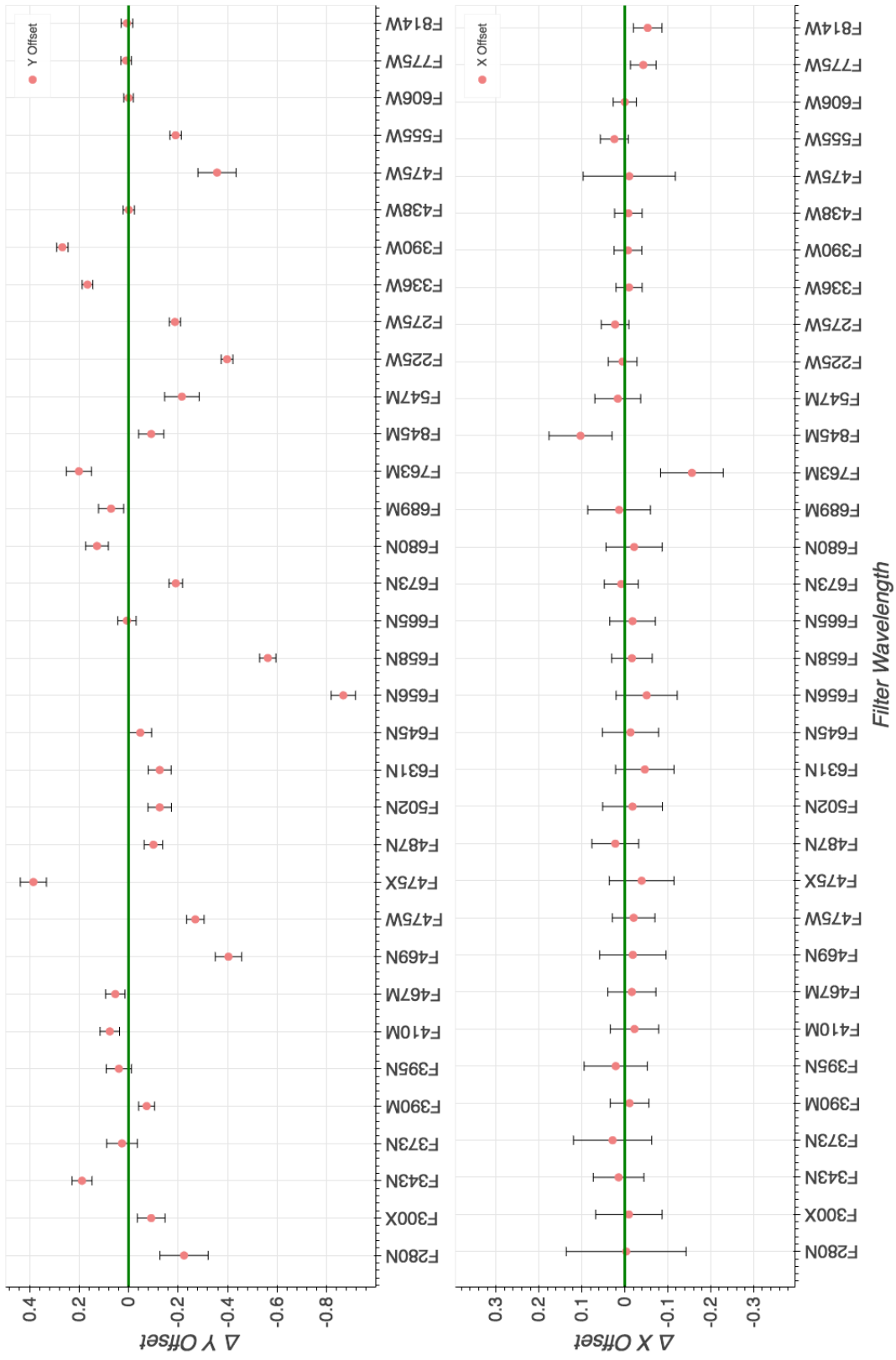


Figure 3: Difference of the average Y-offset (top) and the average X-Offset (bottom) of each filter with an individual solution available compared to the reference Y-offset and X-Offset of F606W.

at the end of the paper. This general shift is a combination of the X-offset and Y-offset (Eq. 5). In Figure 4, we plot the difference between the measured general centroid shifts of each UVIS filter from the general centroid shifts of F606W - as calculated with Eq. 5 and 6. While the individual general centroid shifts of each UVIS filter are a positive value measuring the overall effects of the X and Y-offsets, we do see examples of negative shift values in Figure 4 as we are subtracting the F606W value to compare the new filter solutions to the previous reference solution. Figure 4 demonstrates the range of differences between each UVIS filters' general shift and the reference filter F606W which underscores the need for individual solutions.

$$general_centroid_shift_{filter} = \frac{\sqrt{X_{shift_{filter}}^2 + Y_{shift_{filter}}^2}}{2} \quad (5)$$

$$\Delta shift_{filter} = general_centroid_shift_{filter} - general_centroid_shift_{F606W} \quad (6)$$

The plot in Figure 4 demonstrates the overall centroid shift of each UVIS filter. These shifts range from 0.4 to -0.87 pixel differences from that of the F606W reference shifts. This demonstrates the need of individual solutions for each UVIS filter to ensure the proper corrections for both the unique geometric distortion and unique filter-dependent low-amplitude distortions in each UVIS filter.

6. Conclusions

The goal of this study was to provide complete distortion calibrations for filters that have not previously been characterized. Previous studies have provided similar calibrations for other more commonly used UVIS filters (Kozhurina-Platais et. al, 2009, 2012, 2013, 2014). The continuing observations of ω Cen in various UVIS filters allows us to continue to improve the accuracy of the calibration of all UVIS images.

The variations in the average X,Y relative plate scales, the X,Y centroid shifts and the general centroid shifts that have been discussed in section 5 are caused by differences in the glass layers due to manufacturing and telescope optical set-up. By providing individual high-order polynomial solutions and filter-dependent look-up tables, we can improve the ability of software such as *TweakReg/Astrodrizzle* to match sources in different images taken in these UVIS filter to a RMS solution as low as 0.05 pixels.

The high order polynomial coefficients are updated in the Instrument Distortion Coefficient Table (IDCTAB) and are applied in the HST-pipeline by the STSDAS package *DrizzlePac/Astrodrizzle*. Before the new polynomials are applied by the package, the filter-dependent distortions are applied using the filter distinct 2D look-up tables (NPOLFILE). We have created and delivered 20 new NPOLFILES for each individual filter and updated the IDCTAB with the 20 new sets of polynomial coefficients. All UVIS observations retrieved from MAST will soon have header information updated with these new reference

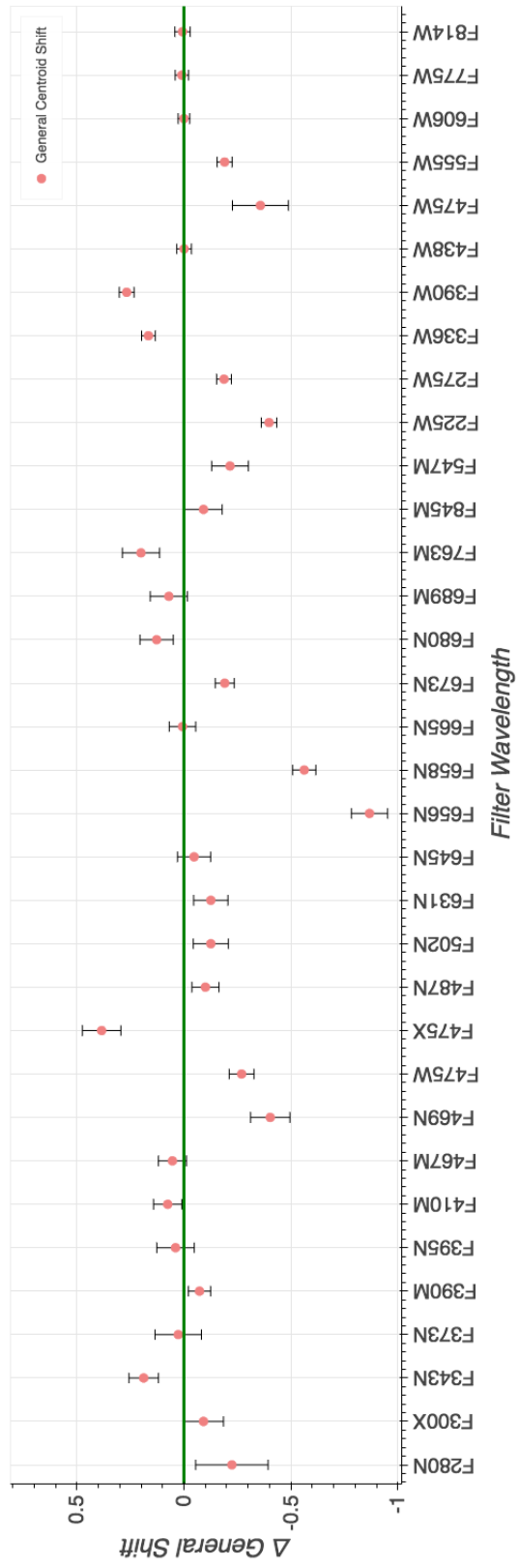


Figure 4: Difference of the shift (diagnostic of the filter wedge) of each updated filter compared to the reference shift of F606W. This shift is a combination of the X, Y shifts plotted in Figure 3.

files. Already downloaded data can be updated at any point using the CRDS bestrefs tool (`crds.bestrefs`).

Acknowledgements

Many thanks to Jay Anderson for his helpful review comments.

References

Fruchter, A., et al., 2009, "The MultiDrizzle Handbook: A Guide for Combining HST Images, Version 3.0", (Baltimore: STScI)

Gonzaga, S., et al., 2012, "The DrizzlePac Handbook, Version 1.0", (Baltimore: STScI)

Kozhurina-Platais, V., Cox, C., McLean, B., "WFC3 SMOV Proposal 11444 - UVIS Geometric Distortion Calibration", WFC3 ISR 2009-33.

Kozhurina-Platais, V., Dulude, M. "WFC3/UVIS and IR Multi-Wavelength Geometric Distortion", WFC3 ISR 2012-07.

Kozhurina-Platais, V., Hammer, D., Dencheva, N., Hack, W. "Astrometric Correction for WFC3/UVIS Lithographic-Mask Pattern", WFC3 ISR 2013-14.

Kozhurina-Platais, V. "Astrometric Correction for WFC3/UVIS Filter-Dependent Component of Distortion", WFC3 ISR 2014-12.

Sabbi, E., "Proposal 11923-UVIS Filter Wedge Check ", WFC3 ISR 2012-001.

Appendix A - Table of Observations

Table 1: Information on the observations used to create the individual calibrations for each filter.

Filter	Rootname	Exposure Time; Date-Obs	POSTARG 1,2	PA_V3	Proposal ID
F280N	id1x09hsq	800.0 secs; 2016-02-01	0.0, 0.0	118.224602	14393
	id1x09htq	800.0 secs; 2016-02-01	40.0, 40.0	118.2397	
	id1x09hvq	850.0 secs; 2016-02-01	-40.0, 40.0	118.216599	
	id1x09hwq	850.0 secs; 2016-02-01	-40.0, -40.0	118.209503	
	id1x09hyq	850.0 secs; 2016-02-01	40.0, -40.0	118.232697	
	id1x09hzq	850.0 secs; 2016-02-01	0.0, 0.0	118.224602	
F343N	id1x10d7q	545.0 secs; 2016-03-25	0.0, 0.0	155.076401	14393
	id1x10d9q	545.0 secs; 2016-03-25	40.0, 40.0	155.083694	
	id1x10dbq	545.0 secs; 2016-03-25	0.0, 40.0	155.072296	

Filter	Rootname	Exposure Time; Date-Obs	POSTARG 1,2	PA_V3	Proposal ID
	id1x10ddq	545.0 secs; 2016-03-25	-40.0, 40.0	155.060898	
	id1x10dfq	510.0 secs; 2016-03-25	-40.0, 0.0	155.065002	
	id1x10dhq	510.0 secs; 2016-03-25	-40.0, -40.0	155.069107	
	id1x10djg	510.0 secs; 2016-03-25	40.0, -40.0	155.091904	
	id1x10dlq	510.0 secs; 2016-03-25	40.0, -40.0	155.091904	
	id1x10dnq	510.0 secs; 2016-03-25	40.0, 0.0	155.087799	
F373N	id1x10dpq	500.0 secs; 2016-03-25	0.0, 0.0	155.076401	14393
	id1x10drq	500.0 secs; 2016-03-25	40.0, 40.0	155.083694	
	id1x10dtq	500.0 secs; 2016-03-25	-40.0, 40.0	155.060898	
	id1x10dvq	500.0 secs; 2016-03-25	0.0, 0.0	155.076401	
	id1x10dxq	500.0 secs; 2016-03-25	-40.0, 40.0	155.060898	
F395N	id1x12i4q	450.0 secs; 2016-02-01	0.0, 0.0	118.301399	14393
	id1x12i6q	450.0 secs; 2016-02-01	40.0, 40.0	118.316498	
	id1x12i8q	450.0 secs; 2016-02-01	-40.0, 40.0	118.293297	
	id1x12iaq	450.0 secs; 2016-02-01	-40.0, -40.0	118.286301	
	id1x12icq	450.0 secs; 2016-02-01	40.0, -40.0	118.309502	
F469N	id1x13ifq	450.0 secs; 2016-02-01	0.0, 0.0	118.340302	14393
	id1x13ihq	450.0 secs; 2016-02-01	40.0, 40.0	118.3554	
	id1x13ijq	450.0 secs; 2016-02-01	-40.0, 40.0	118.332199	
	id1x13ilq	450.0 secs; 2016-02-01	-40.0, -40.0	118.325203	
	id1x13inq	450.0 secs; 2016-02-01	40.0, -40.0	118.348396	
F487N	id1x14btq	450.0 secs; 2016-02-04	0.0, 0.0	120.092903	14393
	id1x14bvq	450.0 secs; 2016-02-04	40.0, 40.0	120.107803	
	id1x14bxq	450.0 secs; 2016-02-04	-40.0, 40.0	120.084396	
	id1x14bzq	450.0 secs; 2016-02-04	-40.0, -40.0	120.078102	
	id1x14c1q	450.0 secs; 2016-02-04	40.0, -40.0	120.101501	
	id1x15wdq	450.0 secs; 2016-02-04	0.0, 0.0	149.028503	
	id1x15wfq	450.0 secs; 2016-02-04	40.0, 40.0	149.037292	
	id1x15whq	450.0 secs; 2016-02-04	-40.0, 40.0	149.013794	
	id1x15wjg	450.0 secs; 2016-02-04	-40.0, -40.0	149.019608	
	id1x15wlq	450.0 secs; 2016-02-04	40.0, -40.0	149.043106	
F502N	id1x11vqq	350.0 secs; 2016-03-17	0.0, 0.0	147.998199	14393
	id1x11vsq	350.0 secs; 2016-03-17	40.0, 40.0	148.007401	
	id1x11vuq	350.0 secs; 2016-03-17	-40.0, 40.0	147.983704	
	id1x11vwq	350.0 secs; 2016-03-17	-40.0, -40.0	147.989105	
	id1x11vyq	350.0 secs; 2016-03-17	40.0, -40.0	148.012695	
F631N	id1x11w0q	350.0 secs; 2016-03-17	0.0, 0.0	147.998199	14393
	id1x11w2q	350.0 secs; 2016-03-17	0.0, 0.0	147.998199	
	id1x11w4q	350.0 secs; 2016-03-17	0.0, 0.0	147.998199	
	id1x11w6q	350.0 secs; 2016-03-17	0.0, 0.0	147.998199	
	id1x11w8q	350.0 secs; 2016-03-17	40.0, -40.0	148.012695	
F645N	id1x16aiq	350.0 secs; 2016-02-01	0.0, 0.0	117.830902	14393

Filter	Rootname	Exposure Time; Date-Obs	POSTARG 1,2	PA_V3	Proposal ID
	id1x16alq	350.0 secs; 2016-02-01	40.0, 40.0	117.849701	
	id1x16aqq	350.0 secs; 2016-02-01	-40.0, 40.0	117.826599	
	id1x16asq	350.0 secs; 2016-02-01	-40.0, -40.0	117.819397	
	id1x16auq	350.0 secs; 2016-02-01	40.0, -40.0	117.842499	
F656N	ibbz01wlq	500.0 secs; 2010-08-28	0.0,0.0	311.836487	11922
	ibbz01wpq	500.0 secs; 2010-08-28	40.0,40.0	311.823608	
	ibbz01wvq	500.0 secs; 2010-08-28	-40.0,40.0	311.847809	
	ibbz01wxq	500.0 secs; 2010-08-28	-40.0,-40.0	311.849213	
	ibbz01wzq	500.0 secs; 2010-08-28	40.0,-40.0	311.825104	
	icqx07chq	350.0 secs; 2015-03-07	40.0,-40.0	133.110794	14031
F658N	iben01i3q	350.0 secs; 2010-09-03	0.0,0.0	316.290588,	12091
	iben01i4q	350.0 secs; 2010-09-03	-8.0,8.0	316.293091	
	iben01i6q	350.0 secs; 2010-09-03	8.0,8.0	316.288208	
	iben01i8q	350.0 secs; 2010-09-03	8.0,-8.0	316.288086	
	iben01iaq	350.0 secs; 2010-09-03	-8.0,-8.0	316.292999	
	iben01icq	350.0 secs; 2010-09-03	-24.0,-8.0	316.297791	
F665N	id1x16axq	350.0 secs; 2016-02-01	0.0, 0.0	117.834503	14393
	id1x16azq	350.0 secs; 2016-02-01	40.0, 40.0	117.849701	
	id1x16bsq	350.0 secs; 2016-02-01	40.0, 40.0	117.849701	
	id1x16buq	350.0 secs; 2016-02-01	-40.0, 40.0	117.826599	
	id1x16bxq	350.0 secs; 2016-02-01	-40.0, 40.0	117.826599	
	id1x16bzq	350.0 secs; 2016-02-01	-40.0, -40.0	117.819397	
	id1x16c1q	340.0 secs; 2016-02-01	0.0, -40.0	117.830902	
	id1x16c6q	340.0 secs; 2016-02-01	40.0, -40.0	117.842499	
	id1x16cvq	340.0 secs; 2016-02-01	40.0, 0.0	117.8461	
F680N	id1x16czq	330.0 secs; 2016-02-01	0.0, 0.0	117.834503	14393
	id1x16d0q	330.0 secs; 2016-02-01	40.0, -40.0	117.842499	
	id1x16d5q	330.0 secs; 2016-02-01	40.0, 40.0	117.849701	
	id1x16d6q	350.0 secs; 2016-02-01	-40.0, -40.0	117.819397	
	id1x16deq	350.0 secs; 2016-02-01	-40.0, 40.0	117.826599	
F390M	ibm501rlq	350.0 secs; 2010-12-12	0.0,0.0	83.181259	12353
	ibm501rrq	350.0 secs; 2010-12-12	0.0,0.0	83.181259	
	ibm516f9q	350.0 secs; 2011-07-25	0.0,0.0	275.999207	
	ibm516ffq	350.0 secs; 2011-07-25	0.0,0.0	275.999207	
	icqx01thq	400.0 secs; 2015-01-08	0.0,0.0	103.846298	14031
	icqx01tjq	400.0 secs; 2015-01-08	40.0,40.0	103.862999	
	icqx01tlq	400.0 secs; 2015-01-08	0.0,40.0	103.8526	
	icqx01tnq	400.0 secs; 2015-01-08	-40.0,40.0	103.8423	
	icqx01tpq	400.0 secs; 2015-01-08	-40.-40,0.0	103.829697	
	icqx01tvq	400.0 secs; 2015-01-08	0.0,-40.0	103.839996	
	icqx01tzq	400.0 secs; 2015-01-08	40.-40,0.0	103.850403	
F547M	id1x05uyq	425.0 secs; 2016-02-07	0.0, 0.0	121.815598	14393

Filter	Rootname	Exposure Time; Date-Obs	POSTARG 1,2	PA_V3	Proposal ID
	id1x05v0q	425.0 secs; 2016-02-07	40.0, 40.0	121.8302	
	id1x05v2q	425.0 secs; 2016-02-07	-40.0, 40.0	121.806602	
	id1x05v4q	425.0 secs; 2016-02-07	-40.0, -40.0	121.801003	
	id1x05v6q	425.0 secs; 2016-02-07	40.0, -40.0	121.8246	
F763M	id1x07biq	450.0 secs; 2016-02-04	0.0, 0.0	120.053902	14393
	id1x07bkq	450.0 secs; 2016-02-04	40.0, 40.0	120.068802	
	id1x07bmq	450.0 secs; 2016-02-04	-40.0, 40.0	120.045403	
	id1x07boq	450.0 secs; 2016-02-04	-40.0, -40.0	120.039101	
	id1x07bqq	450.0 secs; 2016-02-04	40.0, -40.0	120.0625	
F845M	id1x08ucq	450.0 secs; 2016-02-07	0.0, 0.0	121.700699	14393
	id1x08ueq	450.0 secs; 2016-02-07	40.0, 40.0	121.715302	
	id1x08ugq	450.0 secs; 2016-02-07	-40.0, 40.0	121.691704	
	id1x08uiq	450.0 secs; 2016-02-07	-40.0, -40.0	121.685997	
	id1x08ukq	450.0 secs; 2016-02-07	40.0, -40.0	121.709602	
F475W	ibm501rpq	350.0 secs; 2010-12-12	0.0, 0.0	83.181259	12353
	ibm516fdq	350.0 secs; 2011-07-25	0.0, 0.0	275.999207	
	icqx01trq	450.0 secs; 2015-01-08	-40.0, 40.0	103.846298	14031
	icqx01tpq	350.0 secs; 2015-01-08	0.0, 0.0	103.829697	
	icqx01ttq	350.0 secs; 2015-01-08	0.0, 40.0	103.8526	
	icqx01txq	350.0 secs; 2015-01-08	40.0, 40.0	103.862999	
	icqx01u3q	350.0 secs; 2015-01-08	0.0, -40.0	103.839996	
	icqx01u4q	350.0 secs; 2015-01-08	-40.0, -40.0	103.829697	
	icqx01u6q	350.0 secs; 2015-01-08	-40.0, 40.0	103.8423	
	icqx01u8q	350.0 secs; 2015-01-08	40.0, -40.0	103.850403	
F475X	id1x02p7q	350.0 secs; 2016-02-02	0.0, 0.0	118.885002	14393
	id1x02p9q	350.0 secs; 2016-02-02	40.0, 40.0	118.900101	
	id1x02pbq	350.0 secs; 2016-02-02	-40.0, 40.0	118.876801	
	id1x02pdq	350.0 secs; 2016-02-02	-40.0, -40.0	118.870003	
	id1x02pfq	350.0 secs; 2016-02-02	40.0, -40.0	118.893303	
F600LP	id1x01ilq	375.0 secs; 2015-12-12	0.0, 0.0	81.967209	14393
	id1x01ioq	375.0 secs; 2015-12-11	40.0, 40.0	81.984169	
	id1x01itq	375.0 secs; 2015-12-12	-40.0, 40.0	81.96965	
	id1x01iwq	375.0 secs; 2015-12-12	-40.0, -40.0	81.950249	
	id1x01izj	375.0 secs; 2015-12-12	40.0, -40.0	81.96476	
	id1x01j1q	375.0 secs; 2015-12-12	0.0, 0.0	81.967209	

Appendix B - Residual Plots for Calibrated Filters

Narrow Filters:

F280N

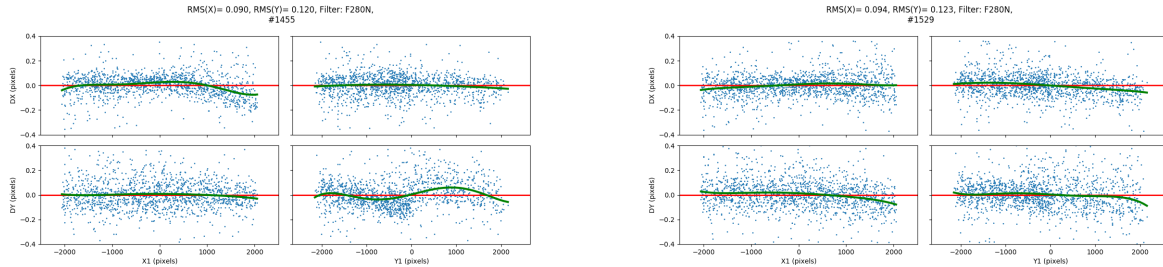


Figure 5: **Left:** TweakReg residuals for the matching of stars in the same image of ω Cen taken with F606W and F280N solved using just F606W distortion solutions on both. **Right:** TweakReg residuals for the matching of stars in the same image of ω Cen taken with F606W and F280N solved using individual distortion solutions for both.

F343N

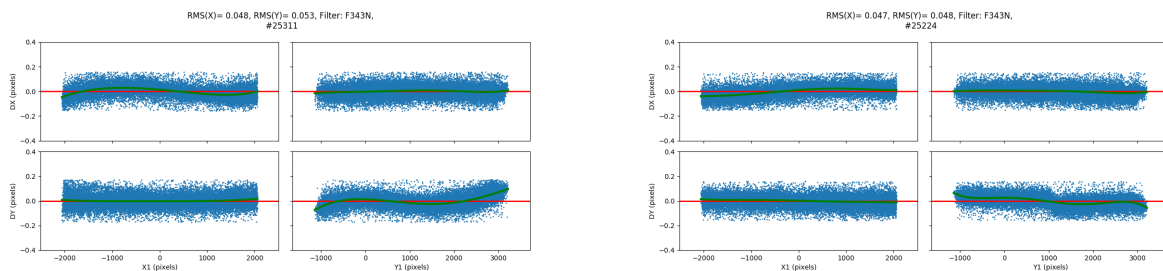


Figure 6: The same comparison as above, except for F343N.

F373N

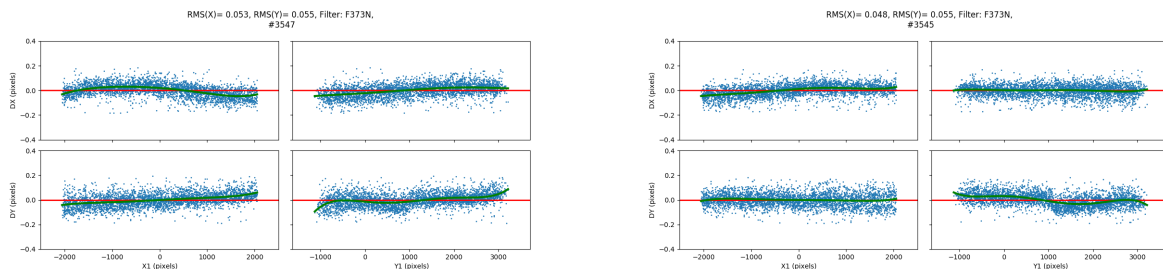


Figure 7: The same comparison as above, except for F373N.

F395N

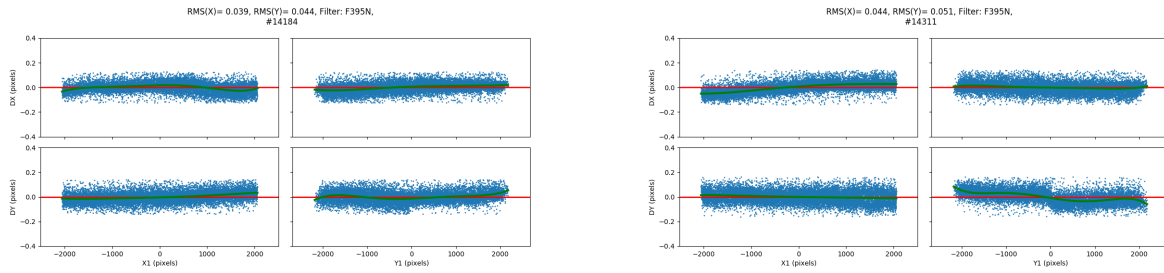


Figure 8: The same comparison as above, except for F395N.

F469N

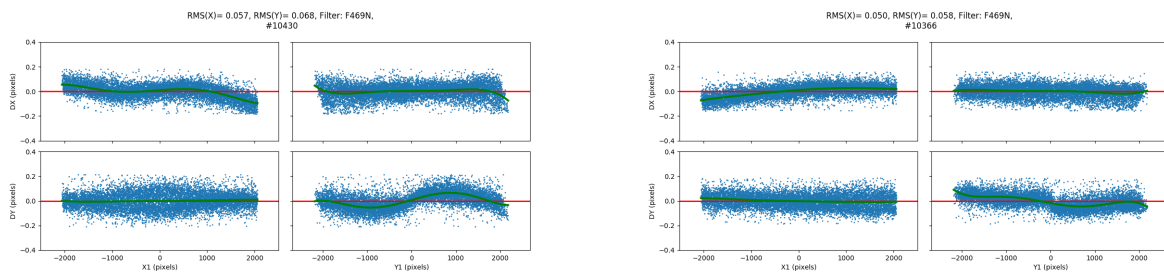


Figure 9: The same comparison as above, except for F469N.

F487N

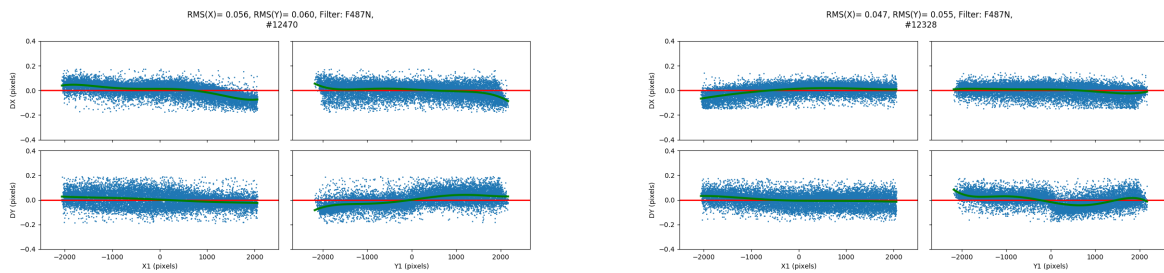


Figure 10: The same comparison as above, except for F487N.

F502N

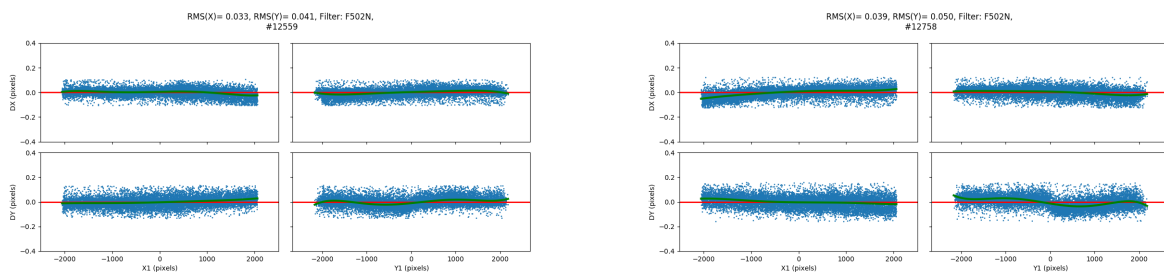


Figure 11: The same comparison as above, except for F502N.

F631N

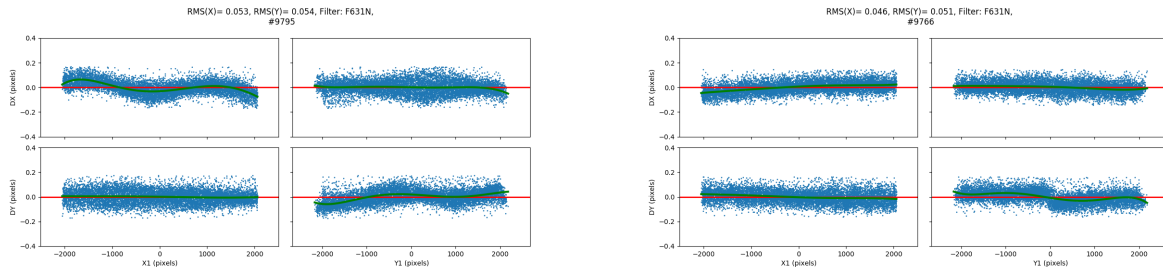


Figure 12: The same comparison as above, except for F631N.

F645N

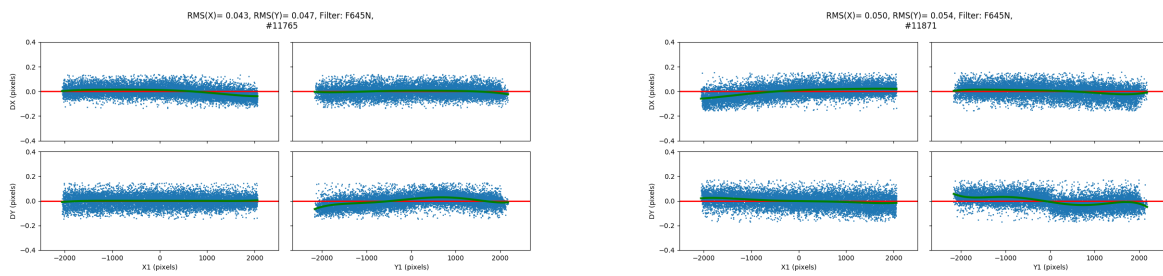


Figure 13: The same comparison as above, except for F645N.

F656N

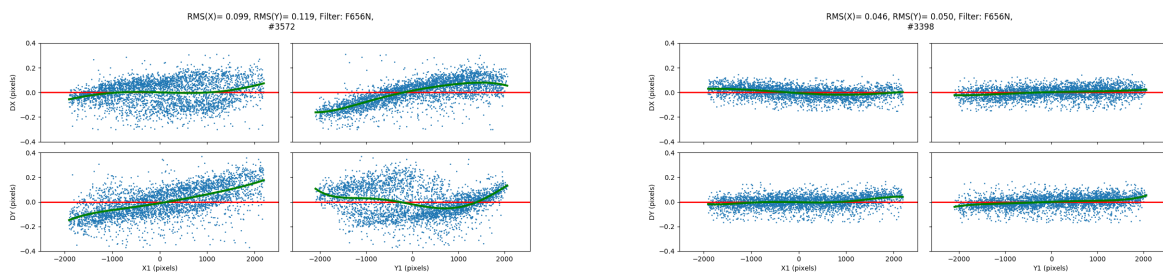


Figure 14: The same comparison as above, except for F656N.

F658N

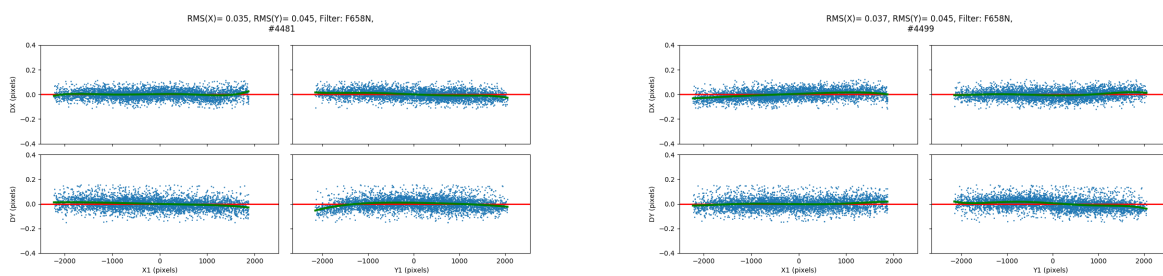


Figure 15: The same comparison as above, except for F658N.

F665N

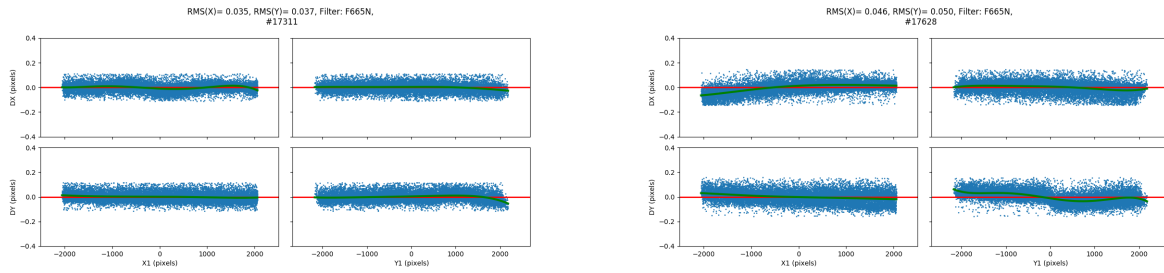


Figure 16: The same comparison as above, except for F665N.

F680N

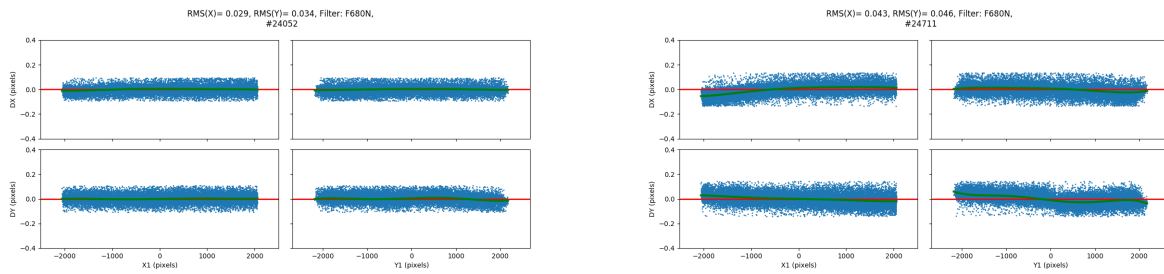


Figure 17: The same comparison as above, except for F680N.

Medium Filters:

F390M

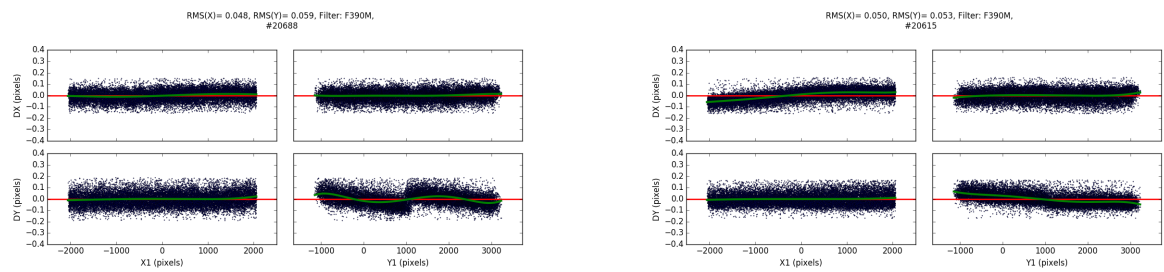


Figure 18: The same comparison as above, except for F390M.

F547M

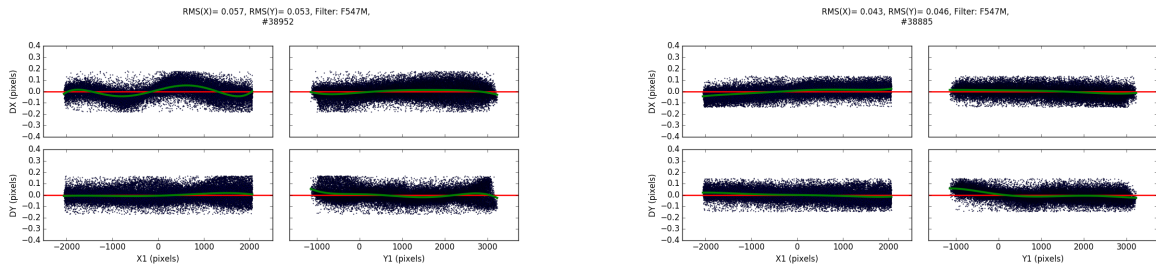


Figure 19: The same comparison as above, except for F547M.

F763M

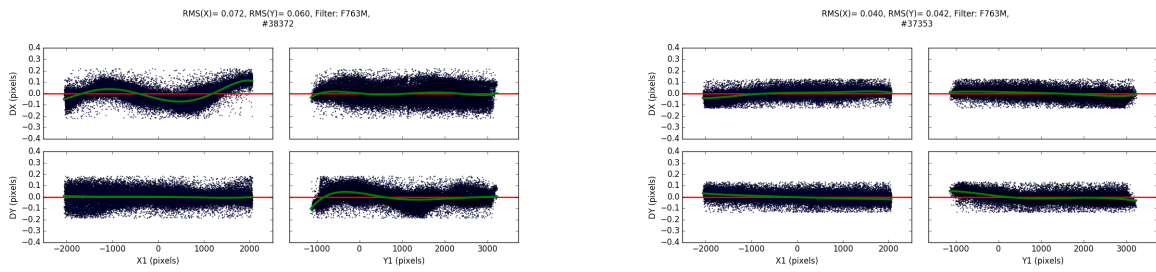


Figure 20: The same comparison as above, except for F763M.

F845M

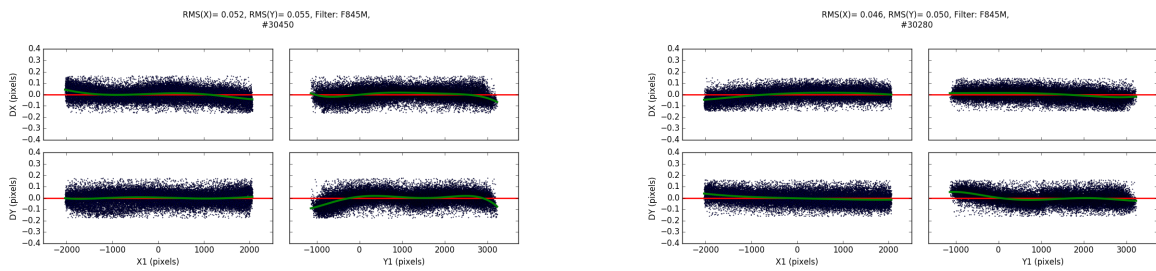


Figure 21: The same comparison as above, except for F845M.

Unique Filters:

F475W

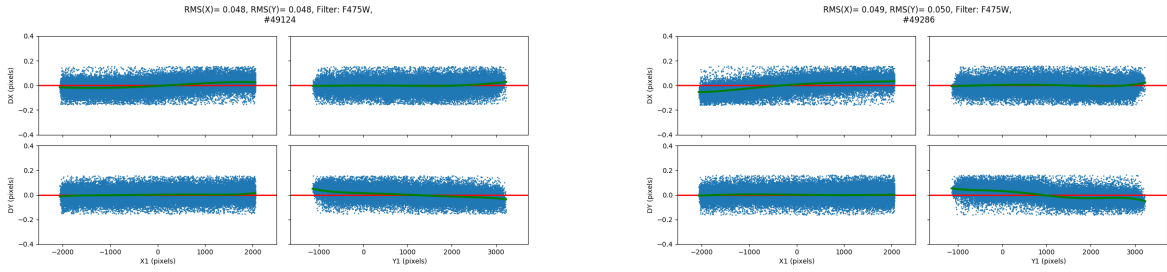


Figure 22: The same comparison as above, except for F475W.

F475X

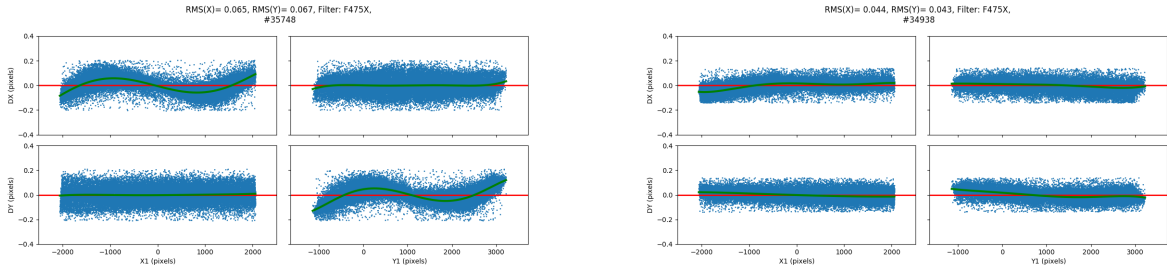


Figure 23: The same comparison as above, except for F475X.

F600LP

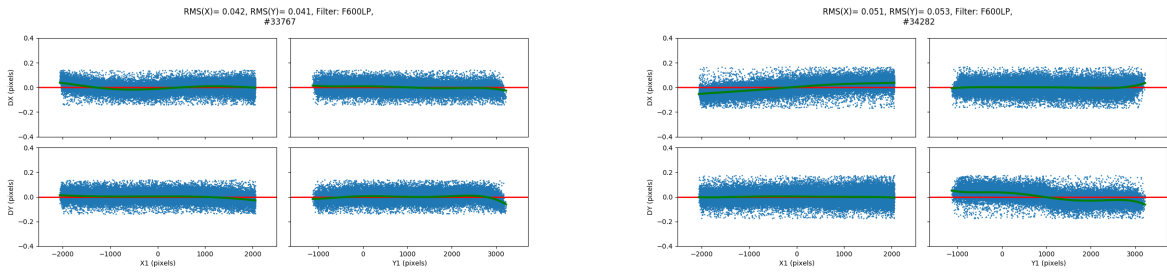


Figure 24: The same comparison as above, except for F600LP.